Puffin: Overview

April 26, 2016

The code Puffin[1] is an FEL simulation code - it is a so-called 'unaveraged' FEL code, which has an enhanced resolution over that of more conventional averaged codes. It can model fast changes in both the electron beam and radiation temporal structure, and can model any frequency (limited by the Niquist condition). The code has undergone many improvements and extended its functionality since the initial publication in [1]. It no longer uses an external linear solver package, and some of the scaling has changed - see below. Before, only the electron beam was distributed in memory across MPI nodes - now both the field and the beam are stored and solved in parallel, enabling the modelling of extremely large systems.

Puffin can now output data in hdf5 format, with VizSchema metadata added to allow visualization with *e.g.* Visit on a cluster. Some visualization examples are shown below in figures 1 and 2.

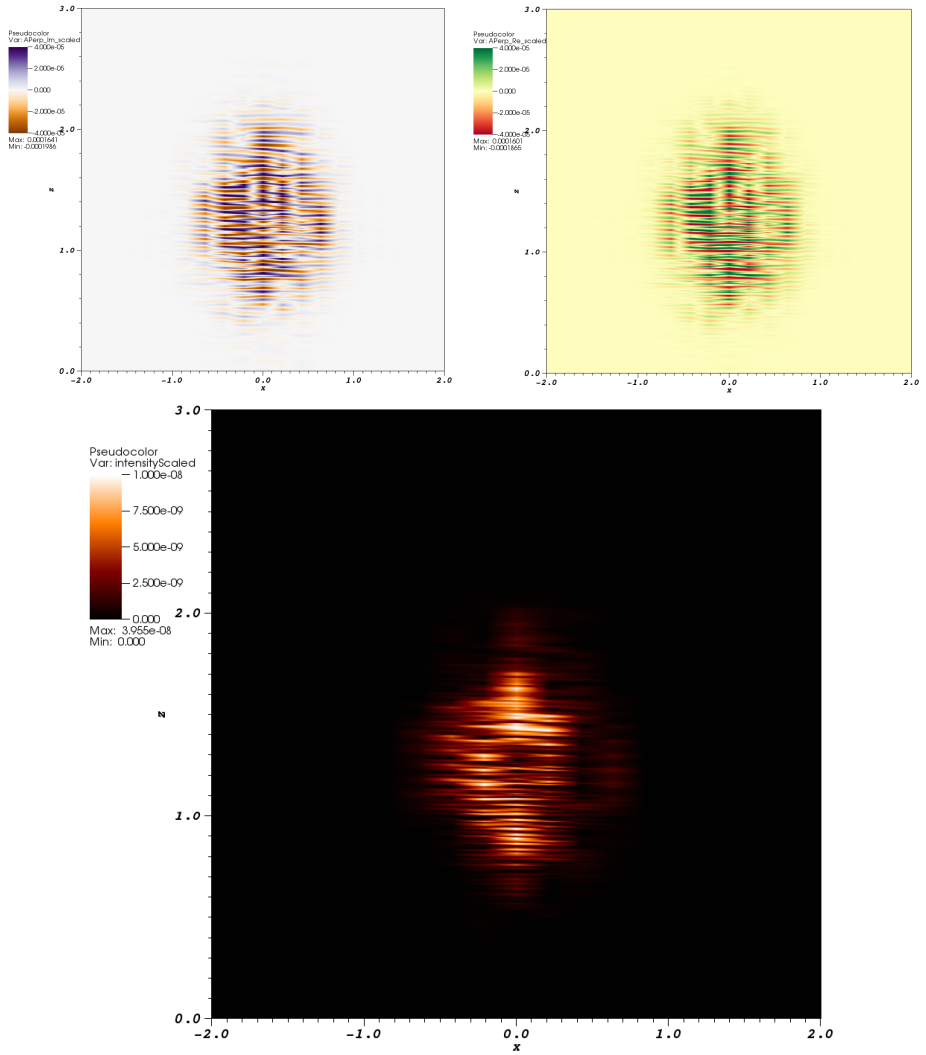

Figure 1: Radiated spontaneous field from Puffin in the first few undulator periods - x (top left) and y (top right) polarized fields, and instantaneous intensity (bottom), at $y = 0$. Radiation is propagating in the negative z direction (the vertical axis). One can see the noisy phase of the radiation in both transverse (x) and temporal (z) directions, which is due to the shot-noise of the electron beam.

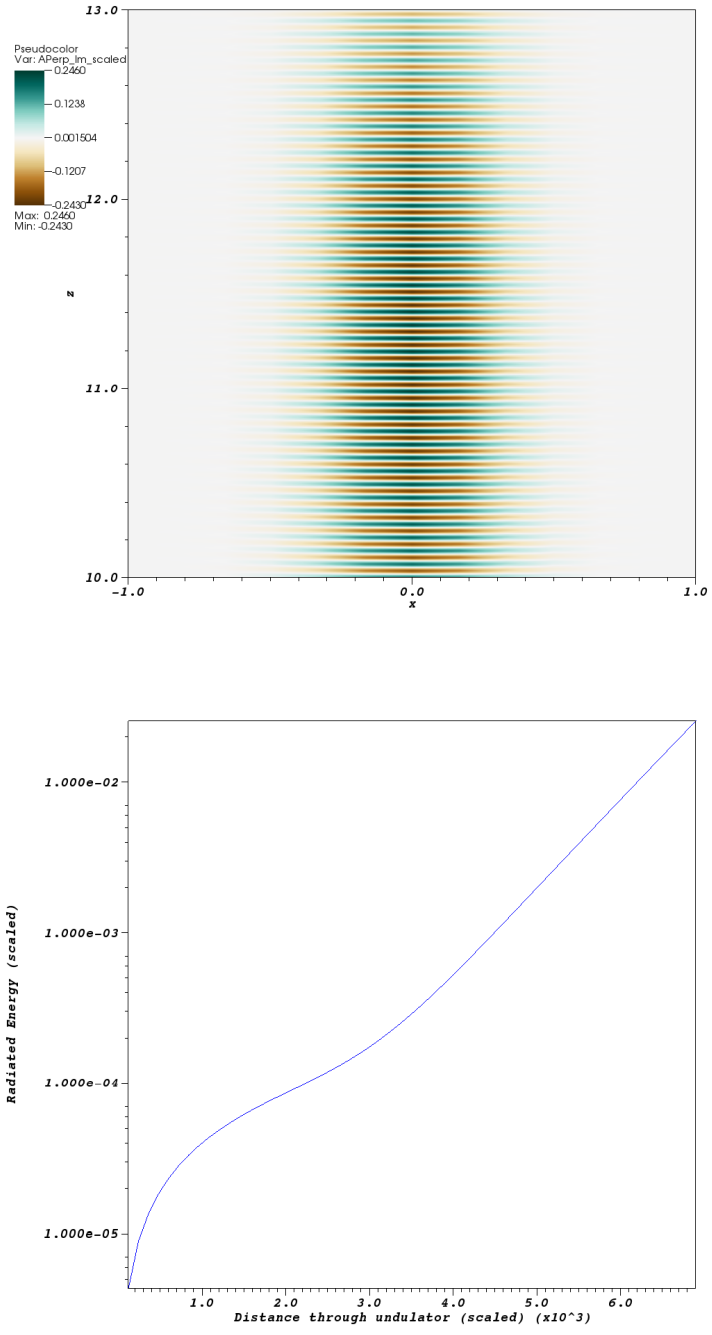

Figure 2: Radiated field from Puffin after amplification in the undulator - x polarized field (top). Radiated energy vs scaled distance through the undulator is on the bottom. Observe the noise from the previous figure has disappeared; the amplification process cause the electrons to align and radiate in phase.

1 Overview

The system of equations solved by Puffin have been altered from those described in [1]. They are now:

$$\Big[\frac{1}{2}\Big(\frac{\partial^2}{\partial\bar{x}^2}+\frac{\partial^2}{\partial\bar{y}^2}\Big)-\frac{\partial^2}{\partial\bar{z}\partial\bar{z}_2}\Big]A_\perp=-\frac{1}{\bar{n}_p}\frac{\partial}{\partial\bar{z}_2}\sum_{j=1}^{N}\frac{\bar{p}_{\perp j}}{\Gamma_j}(1+\eta p_{2j})\delta^3(\bar{x}_j,\bar{y}_j,\bar{z}_{2j}) \tag{1}$$

$$\frac{d\bar{p}_{\perp j}}{d\bar{z}}=\frac{1}{2\rho}\Big[i\alpha b_\perp-\frac{\eta p_{2j}}{\kappa^2}A_\perp\Big]-i\kappa\frac{\bar{p}_{\perp j}}{\Gamma_j}(1+\eta p_{2j})\alpha b_z \tag{2}$$

$$\frac{d\Gamma_j}{d\bar{z}}=-\rho\frac{(1+\eta p_{2j})}{\Gamma_j}(\bar{p}_{\perp j}A^*_{\perp j}+c.c.) \tag{3}$$

$$\frac{d\bar{z}_{2j}}{d\bar{z}}=p_{2j} \tag{4}$$

$$\frac{d\bar{x}_j}{d\bar{z}}=\frac{2\rho\kappa}{\sqrt{\eta}\Gamma_j}(1+\eta p_{2j})\Re(\bar{p}_{\perp j}) \tag{5}$$

$$\frac{d\bar{y}_j}{d\bar{z}}=-\frac{2\rho\kappa}{\sqrt{\eta}\Gamma_j}(1+\eta p_{2j})\Im(\bar{p}_{\perp j}). \tag{6}$$

Scaled parameters are:-

$$\bar{z}_{2j}=\frac{ct_j-z}{l_c},\qquad \bar{z}=\frac{z}{l_g},$$

$$\bar{p}_\perp=\frac{p_\perp}{mca_u},\qquad A_\perp=\frac{e\kappa l_g}{\gamma_0 mc^2}E_\perp,$$

$$(\bar{x},\bar{y})=\frac{(x,y)}{\sqrt{l_g l_c}},\qquad l_g=\frac{\lambda_w}{4\pi\rho},$$

$$l_c=\frac{\lambda_r}{4\pi\rho},\qquad \Gamma_j=\frac{\gamma_j}{\gamma_0},$$

$$\rho=\frac{1}{\gamma_0}\left(\frac{a_u\omega_p}{4ck_u}\right)^{2/3},\qquad a_u=\frac{eB_0}{mck_u},$$

$$\kappa=\frac{a_u}{2\rho\gamma_0},\qquad b_\perp=b_x-ib_y,$$

B_0 is the peak magnetic field in the wiggler. $\omega_p = \sqrt{e^2 n_p/\epsilon_0 m}$ is the (non-relativistic) plasma frequency, and n_p is the peak spatial number density of the electron beam ($N_e/\delta_x\delta_y\delta_z$). $E_\perp = E_x - iE_y$ are the x and y radiation electric field vectors. γ_0 is the reference energy (Lorentz factor), which is usually taken as the mean beam energy.

The scaled reference velocity,

$$\eta = \frac{1-\beta_{zr}}{\beta_{zr}} = \frac{\lambda_r}{\lambda_u} = \frac{l_c}{l_g}, \tag{7}$$

where β_{zr} is some reference velocity scaled to c, which is sensible (but not, strictly speaking, necessary) to take as the mean longitudinal electron velocity in the wiggler, so that

$$\beta_{zr} = \sqrt{1 - \frac{1}{\gamma_0^2}\Big(1 + \bar{a}_u^2\Big)}, \tag{8}$$

where $\bar{a}_u$ is the rms undulator parameter. This defines the velocity at which the electrons travel in the scaled $\bar{z}_2$ frame. More generally, η describes an *ideal* resonance condition - electrons resonant with wavelength λ_r will travel with velocity $p_2 = 1$ through the $\bar{z}_2$ frame.

p_{2j} may be worked out analytically from

$$p_{2j} = \frac{1}{\eta}\Big[\Big(1 - \frac{(1 + a_u^2|\bar{p}_{\perp j}|^2)}{\gamma_r^2\Gamma_j^2}\Big)^{-1/2} - 1\Big] \tag{9}$$

at each step. It is NOT output from Puffin.

Outputs from Puffin are the scaled radiation field $A_\perp$, electron phase space coords $\bar{x}, \bar{y}, \bar{z}_2, \bar{p}_\perp, \Gamma$, and scaled distance through the undulator $\bar{z}$. The normalized electron weights are in the file NormChiDataFile.dat (normalised to the peak *spatial* (3D) density).

Compared to the original Puffin paper [1], now the peak magnetic fields are used to scale the system of eqns (as opposed to the rms values used previously). Previously (*e*.g. as described in [1]), the energy exchange was

modelled through the scaled longitudinal velocity p_2. This was problematic in multiple ways from a computational point of view, since p_2 is a function of the energy, p_x and p_y, so that the same quantity was essentially being calculated twice, leading to large errors in some cases. The energy exchange is instead now modelled directly through the scaled variable $\Gamma_j = \gamma_j/\gamma_r$, meaning smaller numerical errors and enabling a significantly larger step size.

The formalism for including a variation in the magnetic undulator field, so that $B_0(\bar{z})$ now varies, was included in [2], and is varied using the parameter $\alpha(\bar{z}) = \dfrac{B_0(\bar{z})}{B_0(\bar{z}=0)}$.

In the most basic form, the input requires 3 files - a 'main' input file for parameters, numerical integration, and description of the field mesh, a 'beam' input file descibing the electron beam, and a 'seed' input file describing the radiation seed. Optionally, a lattice file can be used to setup an undulator-chicane lattice.

1.1 Parameters

Description of parameters:-

sRho

ρ, the FEL parameter. This specifies the scaling of the system. It does **not** have to be strictly correct - it only descibes the scaling. The simulation can be performed, and the system may be scaled back to SI units using the supplied scripts (NOT SUPPLIED YET!!). If it is correct, however (meaning, it has been calculated from the beam and undulator parameters input), then the scaled notation becomes physically relevant. For an ideal, 1D system, the system should saturate at intensity $|A|^2 \approx 1$, and the system should be firmly in the high or exponential gain regime at $\bar{z} \approx 2 - 3$. This allows one to see how efficiently the system is lasing w.r.t its ideal case.

saw

a_u, the undulator parameter defined with the peak on-axis magnetic field.

sgamma_r

γ_0, the reference (usually the mean) beam energy.

lambda_w

λ_u, the undulator, or wiggler, period.

zundType

Allows one to select from a choice of undulators. Choices are 'curved', 'planepole', and 'helical', described analytically below. If neither of these are chosen, then the default elliptical undulator is chosen, with polarization specified by u_x and u_y.

sux, suy

u_x and u_y - the relative peak magnetic field of the undulator in each transverse polarization. Usually, at least one should be = 1, and the other between 0 (planar) and 1 (helical). If they are not defined, the default is helical, $u_x = u_y = 1$.

1.2 3D Magnetic Fields

The undulator is modelled analytically, and the model must include the fast wiggle motion. Puffin may be modified in the future to allow a map of the undulator field to be input. For now, there are a few generic undulator model employed. The magnetic fields for use in Puffin are the helical, plane-pole, and canted-pole undulator fields discussed in [3], which in the scaled notation here are:-

helical

$$b_x = \cos(\bar{z}/2\rho) \tag{10}$$

$$b_y = \sin(\bar{z}/2\rho) \tag{11}$$

$$b_z = \frac{\sqrt{\eta}}{2\rho}(-\bar{x}\sin(\bar{z}/(2\rho)) + \bar{y}\cos(\bar{z}/(2\rho))) \tag{12}$$

plane-pole

$$b_x = 0 \tag{13}$$

$$b_y = \cosh((\sqrt{\eta}/2\rho)\bar{y})\sin(\bar{z}/2\rho) \tag{14}$$

$$b_z = \sinh((\sqrt{\eta}/2\rho)\bar{y})\cos(\bar{z}/(2\rho) \tag{15}$$

canted-pole

$$b_x = \frac{\bar{k}_{\beta x}}{\bar{k}_{\beta y}}\sinh(\bar{k}_{\beta x}\bar{x})\sinh(\bar{k}_{\beta y}\bar{y})\sin(\bar{z}/2\rho) \tag{16}$$

$$b_y = \cosh(\bar{k}_{\beta x}\bar{x})\cosh(\bar{k}_{\beta y}\bar{y})\sin(\bar{z}/2\rho) \tag{17}$$

$$b_z = \frac{\sqrt{\eta}}{2\rho\bar{k}_{\beta x}}\cosh(\bar{k}_{\beta x}\bar{x})\sinh(\bar{k}_{\beta y}\bar{y})\cos(\bar{z}/2\rho) \tag{18}$$

variably polarized elliptical

$$b_x = u_x\cos(\bar{z}/2\rho) \tag{19}$$

$$b_y = u_y\sin(\bar{z}/2\rho) \tag{20}$$

$$b_z = \frac{\sqrt{\eta}}{2\rho}(u_x\bar{x}\sin(\bar{z}/(2\rho)) + u_y\bar{y}\cos(\bar{z}/(2\rho))) \tag{21}$$

In the 1D approximation, $b_z = 0$.

All of the above have an associated 'natural' focusing channel, which arises from from the off-axis variation in the magnetic fields. This motion arises naturally when numerically solving the equations, and is not superimposed upon the electron motion.

1.3 Undulator Ends

The undulators also include entry and exit tapers, and they may be switched on or off in the input file with the flag **qUndEnds**. Setting this to true will model a smooth taper up and down of the undulator magnetic fields in the first and last 2 periods of the undulator, taking the form of a $\cos^2$. If they are switched off, the beam is artificially initialized with an 'expected' initial condition in the transverse coordinates for that undulator. Including these ends will model a more realistic and natural entry and exit from the undulator, and will reduce CSE effects from the shape of the wiggler.

The precise description of the undulator ends are as follows. Note the presence of corrective terms in addition to the main $\cos^2$ term, which ensure the beam oscillates close to the axis. (Note also the very small non-zero initial $z-$magnetic field in each case, which we find has no noticable deleterious effects in practice.)

Helical Front

$$b_x = \frac{1}{4}\sin(\bar{z}/16\rho)\cos(\bar{z}/16\rho)\sin(\bar{z}/2\rho) + \sin^2(\bar{z}/16\rho)\cos(\bar{z}/2\rho) \tag{22}$$

$$b_y = -\frac{1}{4}\sin(\bar{z}/16\rho)\cos(\bar{z}/16\rho)\cos(\bar{z}/2\rho) + \sin^2(\bar{z}/16\rho)\sin(\bar{z}/2\rho) \tag{23}$$

$$\begin{aligned} b_z = \frac{\sqrt{\eta}}{2\rho}\Big[\bar{x}\Big(&\frac{1}{32}\cos(\bar{z}/8\rho)\sin(\bar{z}/2\rho) + \frac{1}{4}\sin(\bar{z}/8\rho)\cos(\bar{z}/2\rho) \\ &- \sin^2(\bar{z}/16\rho)\sin(\bar{z}/2\rho)\Big) \\ \bar{y}\Big(&-\frac{1}{32}\cos(\bar{z}/8\rho)\cos(\bar{z}/2\rho) + \frac{1}{4}\sin(\bar{z}/8\rho)\sin(\bar{z}/2\rho) \\ &+ \sin^2(\bar{z}/16\rho)\cos(\bar{z}/2\rho)\Big)\Big] \end{aligned} \tag{24}$$

Helical Back

$$b_x = -\frac{1}{4}\cos(\bar{z}/16\rho)\sin(\bar{z}/16\rho)\sin(\bar{z}/2\rho) + \cos^2(\bar{z}/16\rho)\cos(\bar{z}/2\rho) \tag{25}$$

$$b_y = \frac{1}{4}\cos(\bar{z}/16\rho)\sin(\bar{z}/16\rho)\cos(\bar{z}/2\rho) + \cos^2(\bar{z}/16\rho)\sin(\bar{z}/2\rho) \tag{26}$$

$$\begin{aligned} b_z = \frac{\sqrt{\eta}}{2\rho}\Big[\bar{x}\Big(&-\frac{1}{32}\cos(\bar{z}/8\rho)\sin(\bar{z}/2\rho) - \frac{1}{4}\sin(\bar{z}/8\rho)\cos(\bar{z}/2\rho) \\ &- \cos^2(\bar{z}/16\rho)\sin(\bar{z}/2\rho)\Big) \\ \bar{y}\Big(&\frac{1}{32}\cos(\bar{z}/8\rho)\cos(\bar{z}/2\rho) - \frac{1}{4}\sin(\bar{z}/8\rho)\sin(\bar{z}/2\rho) \\ &+ \cos^2(\bar{z}/16\rho)\cos(\bar{z}/2\rho)\Big)\Big] \end{aligned} \tag{27}$$

Plane-Pole Front

$$b_x = 0, \tag{28}$$

$$b_y = \cosh(\sqrt{\eta}\bar{y}/2\rho)\Big[-\frac{1}{4}\sin(\bar{z}/16\rho)\cos(\bar{z}/16\rho)\cos(\bar{z}/2\rho) + \sin^2(\bar{z}/16\rho)\sin(\bar{z}/2\rho)\Big], \tag{29}$$

$$\begin{aligned} b_z = \sinh(\sqrt{\eta}\bar{y}/2\rho)\Big[&-\frac{1}{32}\cos(\bar{z}/8\rho)\cos(\bar{z}/2\rho) + \\ &\frac{1}{4}\sin(\bar{z}/8\rho)\sin(\bar{z}/2\rho) + \sin^2(\bar{z}/16\rho)\cos(\bar{z}/2\rho)\Big], \end{aligned} \tag{30}$$

Plane-Pole Back

$$b_x = 0, \tag{31}$$

$$b_y = \cosh(\sqrt{\eta}\bar{y}/2\rho)\Big[\frac{1}{4}\sin(\bar{z}/16\rho)\cos(\bar{z}/16\rho)\cos(\bar{z}/2\rho) + \cos^2(\bar{z}/16\rho)\sin(\bar{z}/2\rho)\Big], \tag{32}$$

$$\begin{aligned} b_z = \sinh(\sqrt{\eta}\bar{y}/2\rho)\Big[&\frac{1}{32}\cos(\bar{z}/8\rho)\cos(\bar{z}/2\rho) - \\ &\frac{1}{4}\sin(\bar{z}/8\rho)\sin(\bar{z}/2\rho) + \cos^2(\bar{z}/16\rho)\cos(\bar{z}/2\rho)\Big]. \end{aligned} \tag{33}$$

Curved-Pole Front

$$b_x = \frac{\bar{k}_{\beta x}}{\bar{k}_{\beta y}} \sinh(\bar{k}_{\beta x}\bar{x}) \sinh(\bar{k}_{\beta y}\bar{y}) \Big[-\frac{1}{8} \sin(\bar{z}/8\rho) \cos(\bar{z}/2\rho) + \sin^2(\bar{z}/16\rho) \sin(\bar{z}/2\rho) \Big], \tag{34}$$

$$b_y = \cosh(\bar{k}_{\beta x}\bar{x}) \cosh(\bar{k}_{\beta y}\bar{y}) \Big[-\frac{1}{8} \sin(\bar{z}/8\rho) \cos(\bar{z}/2\rho) + \sin^2(\bar{z}/16\rho) \sin(\bar{z}/2\rho) \Big], \tag{35}$$

$$b_z = \frac{\sqrt{\eta}}{2\rho \bar{k}_{\beta y}} \cosh(\bar{k}_{\beta x}\bar{x}) \sinh(\bar{k}_{\beta y}\bar{y}) \Big[-\frac{1}{32} \cos(\bar{z}/8\rho) \cos(\bar{z}/2\rho) + \frac{1}{4} \sin(\bar{z}/8\rho) \sin(\bar{z}/2\rho) + \sin^2(\bar{z}/16\rho) \cos(\bar{z}/2\rho) \Big]. \tag{36}$$

Curved-Pole Back

$$b_x = \frac{\bar{k}_{\beta x}}{\bar{k}_{\beta y}} \sinh(\bar{k}_{\beta x}\bar{x}) \sinh(\bar{k}_{\beta y}\bar{y}) \Big[\frac{1}{8} \sin(\bar{z}/8\rho) \cos(\bar{z}/2\rho) + \cos^2(\bar{z}/16\rho) \sin(\bar{z}/2\rho) \Big], \tag{37}$$

$$b_y = \cosh(\bar{k}_{\beta x}\bar{x}) \cosh(\bar{k}_{\beta y}\bar{y}) \Big[\frac{1}{8} \sin(\bar{z}/8\rho) \cos(\bar{z}/2\rho) + \cos^2(\bar{z}/16\rho) \sin(\bar{z}/2\rho) \Big], \tag{38}$$

$$b_z = \frac{\sqrt{\eta}}{2\rho \bar{k}_{\beta y}} \cosh(\bar{k}_{\beta x}\bar{x}) \sinh(\bar{k}_{\beta y}\bar{y}) \Big[\frac{1}{32} \cos(\bar{z}/8\rho) \cos(\bar{z}/2\rho) - \frac{1}{4} \sin(\bar{z}/8\rho) \sin(\bar{z}/2\rho) + \cos^2(\bar{z}/16\rho) \cos(\bar{z}/2\rho) \Big]. \tag{39}$$

1.4 Natural Undulator Focusing

Each undulator type has an associated natural focusing wavenumber. In the helical case, the natural betatron wavenumber is

$$\bar{k}_{\beta nx} = \bar{k}_{\beta ny} = \frac{a_w}{2\sqrt{2}\rho\gamma_0}, \tag{40}$$

with γ_0 being the average beam energy (and not necessarily = γ_r)

In the planar case,

$$\bar{k}_{\beta ny} = \frac{a_w}{2\sqrt{2}\rho\gamma_0}. \tag{41}$$

In the canted pole case,

$$\bar{k}_{\beta nx,y} = \frac{a_w \bar{k}_{x,y}}{\sqrt{2\eta}\gamma_0}, \tag{42}$$

where $\bar{k}_{x,y}$ describe the hyperbolic variation in the transverse directions (see eqns (16 - 18)), and must obey

$$\bar{k}_x^2 + \bar{k}_y^2 = \frac{\eta}{4\rho^2} \tag{43}$$

to be physically valid. They determine the focusing strength in the $\bar{x}$ and $\bar{y}$ dimensions. For the case of equal focusing, then,

$$\bar{k}_{\beta nx} = \bar{k}_{\beta ny} = \frac{a_w}{4\rho\gamma_0}. \tag{44}$$

1.5 Strong Beam Focusing

In addition to the natural focusing channel, a constant, 'strong' focussing channel may be utilized, to focus the beam to a smaller transverse area. This is a magnetic field super-imposed upon the wiggler. It may be switched on or off with the flag **qFocussing** in the main input file, and is specified through the use of the variables **sKBetaXSF** and **sKBetaYSF**. It is probably highly artificial - it may be thought of as physically similar to an ion channel. Nevertheless it allows one to obtain strong focusing without using a lattice. It is defined very simply as

$$b_x = \sqrt{\eta}\frac{\bar{k}_{\beta y}^2}{\kappa}\bar{y}_j, \tag{45}$$

$$b_y = -\sqrt{\eta}\frac{\bar{k}_{\beta x}^2}{\kappa}\bar{x}_j \tag{46}$$

If either **sKBetaXSF** or **sKBetaYSF** are not specified, then no focusing channel will be added for that dimension, even if the **qFocussing** flag is true.

Magnetic quads will be added soon.

1.6 Auto beam-matching

The beam, when specified by the 'simple' method (see below) may be matched to the focusing channel automatically with the flag **qMatched_A** in the beam file - the option can be set for each beam. In the scaled notation,

$$\bar{\sigma}_{x,y} = \sqrt{\frac{\rho\bar{\epsilon}_{x,y}}{\bar{k}_{\beta x,y}}} \tag{47}$$

where $\bar{\epsilon}_{x,y} = \epsilon_{x,y}/(\lambda_r/4\pi)$ are the transverse emittances scaled to the so-called Kim criterion.

The spread in the transverse momentum directions is then given by

$$\bar{\sigma}_{px,py} = \frac{\sqrt{\eta}}{2\kappa}\Big\langle\frac{\Gamma}{1+\eta p_2}\Big\rangle\frac{\bar{\epsilon}_{x,y}}{\bar{\sigma}_{x,y}}. \tag{48}$$

where angular brackets indicate the ensemble average of the beam.

If **qFocussing** is true and the strong betatron wavenumber is given, then the strong betatron wavenumber is used to match the beam. Otherwise the beam is auto-matched to the natural focusing channel of the undulator.

1.7 Beam Initialization

There are 3 different ways of defining and initializing the electron beam in Puffin:

1.7.1 Simple

The beam is described in terms of a homogeneous Gaussian function in every dimension. Some simple correlations in energy can be achieved by specifying

an oscillation in the beam energy as a function of $\bar{z}_2$, or as a simple linear energy chirp in $\bar{z}_2$. The beam is generated in Puffin according to this description.

1.7.2 Dist input

The input is composed of a description of temporal slices along the bunch, describing a Gaussian mean and standard deviation in every other dimension for each temporal slice. This information is used to generate the electron beam in Puffin.

1.7.3 Beam input

This method allows one to read in the 6D scaled particle coordinates from a text file. The beam is generated externally. (Arrangement?)

1.8 Field Mesh

References

[1] L.T. Campbell and B.W.J. McNeil, Physics of Plasmas **19**, 093119 (2012)

[2] L T Campbell, B.W.J. McNeil and S. Reiche, New J. Phys. **16** (2014) 103019

[3] E.T. Scharlemann, in High Gain, High Power FELs (edited by R. Bonifacio *et al*) (1989)

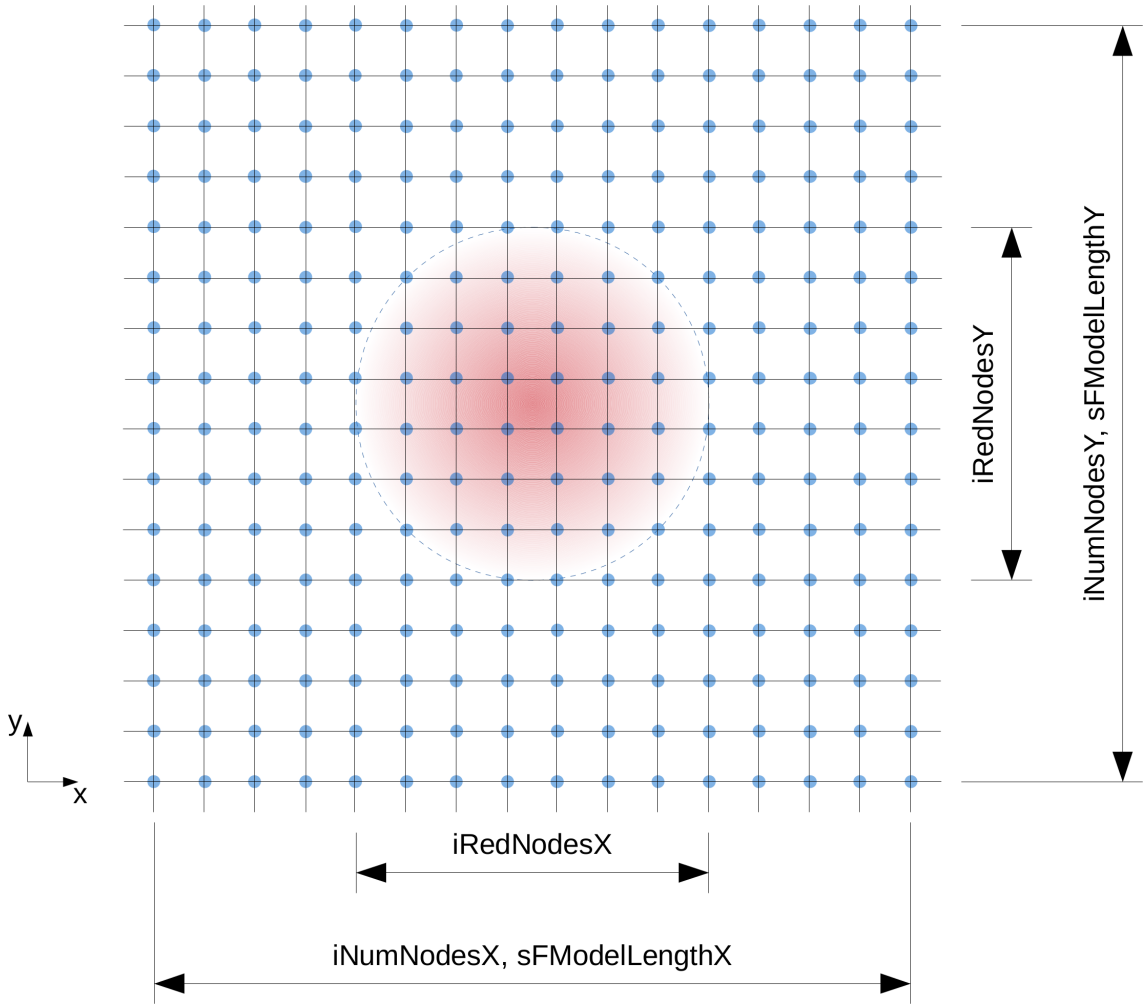

Figure 3: Transverse mesh to model the radiation field - the beam is indicated in red. The mesh may be 'matched' to the mesh initially by specifying the iRedNodes parameters - these specify an inner set of nodes such that the mesh will be setup so that the beam is contained within this number of nodes. This is only an initial condition, but can aid in setting up the mesh.

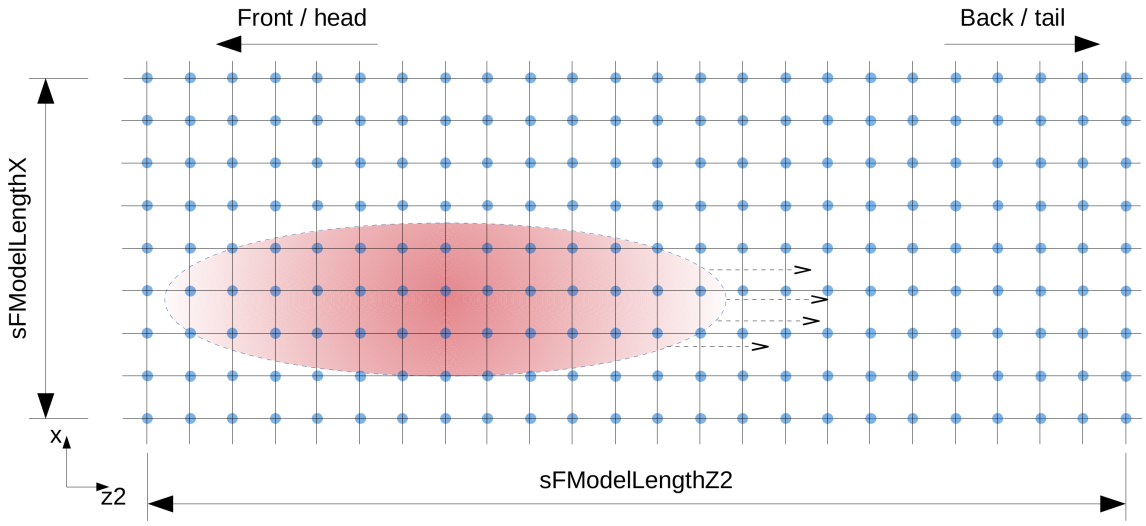

Figure 4: Showing the longitudinal setup of the radiation mesh. The beam is indicated in red. The scaled $\bar{z}_2$ coordinate is defined so that the front of the radiation and beam is to the left. This is the constant radiatioon frame, so the beam slips backwards through the field from left to right. In the lab frame, the beam and radiation propagates from right to left. The full length of the mesh must be large enough to contain the beam through propagation.